Proceedings of the Korean Nuclear Society Spring Meeting
Kwangju, Korea, May 2002

A Study on Hydraulic Resistance of Porous Media Approach for CANDU-6 Moderator Analysis

Churl Yoon, Bo Wook Rhee, and Byung-Joo Min

Korea Atomic Energy Research Institute
150 Dukjin-Dong, Yusong-Gu
Daejeon 305-353, Korea

Abstract

An adequate hydraulic resistance equation is derived from the empirical correlation of frictional pressure drop experiments {Hadaller, et al., 1996}. With implementing hydraulic resistance into the source terms of momentum equations, the better flow pattern and temperature distributions were predicted comparing to the experimental data obtained in the Stern Laboratories Inc. (SLI) in Hamilton, Ontario. The simulations are performed on two test cases; the nominal condition with a mass flow rate of 2.4 kg/s and heat load of 100 kW, and the low-flow condition with a mass flow rate of 2.18 kg/s and heat load of 100 kW. For the simulation, a three-dimensional CFD code, CFX-4 (AEA Technology), is used. The predicted flow pattern and temperature distribution agree well with the experimental measurements and the previous predictions performed by MODTURC_CLAS.

1. Introduction

For some loss of coolant accidents with coincident loss of emergency core cooling in a CANDU-6 reactor, fuel channel integrity depends on the capability of the moderator to act as the ultimate heat sink. Under conditions of high-pressure tube temperature and high coolant pressure, the pressure tube could strain (i.e., balloon) to contact its surrounding Calandria tube. (PT/CT contact) Following contact between the hot pressure tube (PT) and the relatively cold Calandria tube (CT), there is a spike in heat flux to the moderator surrounding the Calandria tube, which leads to sustained CT dryout. The prevention of CT dryout following PT/CT contact depends on available local moderator subcooling. Higher moderator temperatures (lower subcooling) would decrease the margin of the Calandria tubes to dryout in the event of PT/CT contact. In CANDU safety analyses, it is one of major concerns to estimate the local subcooling of moderator inside the Calandria vessel under postulated accident scenarios.

The computer codes that predict moderator temperatures for these accidents have not been

adequately validated, given the small safety margins that exist currently. In the simulation of CANDU-6 moderator circulation and the prediction of local minimum subcooling of the moderator under normal operating conditions and LOCA transients, the resultant velocity fields and temperature predictions are very sensitive to the empirical hydraulic resistance correlations for the porous region which represents a matrix of Calandria tubes.

Huget et al. [1,2] investigated experimentally the moderator circulation and temperature distribution of CANDU moderator under normal operating conditions and other conditions, using 2-dimensional moderator circulation facility at Stern Laboratories. They also provided the predicted velocity fields and temperature for each test case, using MODTURC-CLAS (MODerator TURbulent Circulation Co-Located Advanced Solution).

In the preceding simulations (Yoon, et al. [4]), the CFD moderator analysis model using CFX-4.3 has been validated against ‘SPEL moderator circulation experiments’, with the maximum temperature mismatch of 2.0 ^{o}C.

In this study, a three-dimensional CFD code, CFX-4, is used to simulate the moderator circulation experiments at Stern Lab.

2. Hydraulic Resistance Correlations

To avoid the complexity of generating grids around every heating tube, the porous media approach is applied in the current study. The momentum equation is expressed in the CFX-4.2 manual [5] as

$$\frac{\partial r\ \mathrm{U}}{\partial t} + \nabla \cdot \left(r\ \mathrm{U} \otimes \mathrm{U} \right) = B + \nabla \cdot s \tag{1}$$

Here, B has units of force per unit volume, (N/m^3) in SI units. The hydraulic resistance (impedance) of the porous region is put as a function of local velocity using the subroutines provided by CFX-4.3.

$$B = B_o + B_p U \tag{2}$$

where B_o is velocity-independent body force. B_p(Ns/m^4) is useful to assign flow resistance depending on the local velocity. For an an-isotropic porous region, $B = -RU$, with R = diag(R_x, R_y, R_z).

For axial flow, there is no form drag. The value of R_z may be expressed as below (reference[6]):

$$R_z = \frac{\Delta p_{fric}}{\Delta z} = \frac{f}{D_e} \cdot \frac{r\ u_z}{2} \tag{3}$$

where f is the friction factor and D_e is the hydraulic diameter of flow passage in z-direction.

Hadaller et al.[3] investigated the frictional pressure drop for staggered and in-line tube banks, in which the Reynolds number range is 2000 to 9000 and pitch to tube diameter ratio is 2.16. Also, they concluded that for the given p/d ratio the effect of staggering is not

important. In our study, the tube Reynolds number is around 2000 and p/d ratio is 1.974. Applying the conclusion of Hadaller et al.[3], the resistances depending on the local velocity for transverse flow to the tube matrix are expressed by the correlation below.

$$R_i = \frac{f}{2} \rho g^{4/3} |V_c| \quad , \qquad i = x, y \tag{4}$$

where the quantity $|V|$ is the local magnitude of time-mean fluid velocity, u_i is a velocity component, and f is a loss factor determined from an empirical equation for the losses through tube bundle regions. The ratio of fluid volume to the total volume in the porous region is defined as the volume porosity g. The 1990 Stern lab experiments suggest,

$$f = 4.54 \frac{Re^{-0.172}}{P} \tag{5}$$

where Re is the Reynolds number = $g^{2/3} |V_c| D_{tube} / \nu$, D_{tube} is the diameter of the Calandria tubes, ν is the kinematic viscosity of the fluid, P is the distance between Calandria tube centerlines (pitch), and V_c is the in-core velocity that is calculated at the location of every cell center in the core region and at every iterations.

3. Stern Lab Experiments

The test section of the moderator test facility at Stern Laboratories Inc. (SLI) in Hamilton, Ontario is shown in Fig. 1. The moderator test vessel is a cylinder with a diameter of 2 m and a length of 0.2 m (a thin axial “slice” of CANDU-6 Calandria vessel). It is constructed of transparent polycarbonate walls secured to a steel frame. Light water, representing moderator fluid, is circulated through a low-temperature, low-pressure flow loop by a pump capable of delivering 4 kg/s of flow. The inlet nozzles span the full thickness of the test vessel and are mounted on the circumferential walls so that the jets issue vertically into the vessel at the horizontal centerline. The outlet port at the bottom of the test vessel is a perforated section, which covers the full thickness of the vessel. The orifice meters are used to measure the total loop flow and the flow in each inlet leg. The estimated uncertainty in the flow rate measurements is ± 0.5 % ($2s$).

An array of 440 electrical tube heaters representing fuel channels simulates the reactor core. The lattice pitch of the tube heater array is 0.071 m and the outer diameter of the tubes is 0.033 m. The tubes are fuel designed to act as resistance heaters with a DC power supply or, alternatively, they can be used as electrodes with an AC power supply to induce heat generation in the fluid itself. The power metering is done through separate measurements of the current and voltage in each supply zone. The combined uncertainties are less than one percent.

Fluid velocity measurements in the test vessel are achieved by Laser Doppler Anemometry

(LDA). The LDA system permits measurement of velocities as low as 0.001 m/s at an estimated resolution of 2 percent. Temperature measurements are made using an array of 40 type T thermocouples fixed at various locations in the vessel's centerplane, with most of them concentrated in the top quadrant. The estimated uncertainty in the thermocouple measurements is $\pm$ 0.2°C ($2s$).

The test conditions considered most relevant to the operating conditions of typical CANDU-6 reactor at full power are: a total inlet flow rate of 2.4 kg/s, which corresponds to an inlet velocity of 1 m/s, a total heat input of 100 kW and an outlet temperature of 65°C. These parameters were arrived at by a similarity analysis of the momentum and energy equations. From the various test conditions, two test cases are adapted for the current simulation analysis:

- the nominal-conditions tests, with a flow rate of 2.4 kg/s and a heat load of 100 kW
- a low-flow test, with a flow rate of about 2 kg/s and the nominal heat load of 100 kW.

In nominal-conditions test, a steady flow pattern was sustained for an inlet flow rate of 2.4 kg/s, heater power input of 100 kW, and an inlet temperature of 55°C, resulting in an outlet temperature of 65°C. The observed flow pattern was far from symmetrical. The stagnation point between the inlet jets was at an angle of about 50°C from vertical. The measured maximum temperature in the flow field was 72.4°C at the location near and above the vortex center of the larger recirculation zone. The measured temperature distributions along selected lines in the flow field are shown in fig. 2 ~ fig. 5 in comparison with predictions.

Low-flow test was created in an attempt to establish a buoyancy-dominated flow pattern. The nominal power (100 kW) was applied to the heaters with a less-than-nominal inlet flow rate in the 2.0 to 2.2 kg/s range. The flow pattern was observed to be symmetric and buoyancy-dominated. The jet-driven recirculations were restricted to two small zones close to the inlet nozzles. Although the flow pattern appeared stable, temperatures at the very top of the vessel kept climbing over 85°C, until the test was terminated to prevent damage to the rig. Figure 6 and Fig. 7 show comparison of the simulation results by MODTURC_CLAS and CFX-4.

4. Simulation Results

In this study, a three-dimensional CFD code, CFX-4.3, is used to simulate the Stern lab experiments. This steady state computation using CFX-4.3 was performed in an HP-C3600 workstation. The convergence criteria were the enthalpy residual reduction factor of 10^{-3} and the largest mass residual of 10^{-5}. Because the energy equation and momentum equations are strongly interrelated in this computation, the algebraic multi-grid solver and false time stepping technique were adapted to accelerate converging speed for the energy equation. The number of steady computation iterations was about 30,000~40,000.

Figure 2 shows the simulated velocity field and temperature distribution of nominal condition, using CFX-4. Total flow rate is 2.4 kg/s, the corresponding inlet velocity is 1 m/s, and the inlet temperatures are 55°C. The location of stagnation point appears about 25° from the horizontal centerline, which is lower than 40° predicted by MODTURC_CLAS (Fig. 3). This mismatch might be cause by improper use of turbulent model and associated wall treatment. The maximum temperature calculated by CFX-4 is about 73°C, close to the

measured maximum temperature of 72.4^{o}C.

In the results of the nominal-condition simulation, the flow reversal is observed only one side. The cold injected fluid from the other side inlet nozzle goes all the way through the upper reflector region, guided by the upper circumferential vessel wall. The two injected fluids meet together at the angle of about 25^{o} over the horizontal centerline, where the jet reversal occurs. The reversed fluid goes down to the bottom, guided by the circumferential lower vessel wall. The velocity vectors in most of the core region are a sluggish and skewed upward. In Fig. 2(b), the temperature distribution shows a steep change of temperature around the jet reversal area. In this area, the fluid from the other side nozzle heated during the travel suppresses the cold injected fluid. The hottest spot is located at the upper center area of the core region, which slightly tilts to one side from the vertical centerline.

The comparison of temperatures at the vertical centerline (X = 0 m) in the nominal-condition test is made in Fig. 4. The measured temperature and the predicted temperatures by MODTURC_CLAS computation using 35X21 grid and 51X25 grid are compared with the current simulation result. Figure 5 shows the temperatures at a horizontal line (Y=0.57 m) in the nominal-condition test. The predictions agree well with the measurements in the upper core region, but not quite well in the central core region.

Figure 6 and Fig. 7 present the flow pattern and isotherms predicted for low-flow test. The cold injected fluid through the inlet nozzles changes its direction downward due to the suppression of hot fluid from the top of the test vessel. The reversed fluid goes down to the bottom, guided by the circumferential lower vessel wall. Most of these cold fluids at the bottom go out through the outlet, while some go up into the vacancy that is created by the elevation of heated fluid inside the porous region. Inside the central porous region, the elevation speed of hot fluid induced by buoyancy forces is relatively slow because of the hydraulic resistance. In Fig. 6(b), temperature distribution shows a steep change of temperature around the jet reversal area, where cold fluid from the inlet jet and hot fluid from the top meet together.

5. Conclusions

In the current study, some improvements in implementing the empirical hydraulic resistance correlation are made. One is that the local magnitude of time-mean fluid velocity, $|V|$, should be distinguished from the free stream velocity, which was used in the empirical correlation for hydraulic resistance of the porous region. The other is that the friction coefficient reduction factor, R_f, depends on the attack angle, which is the angle between the flow direction and the axis of tube bank. In current study, cross-sectional component and axial component of flow velocity vector are separated. Therefore, the friction coefficient reduction factor is not appeared in the equations.

By the corrected empirical correlation for porous region hydraulic resistance, the more realistic flow pattern and temperature prediction were obtained using CFX-4 CFD code. But, the local mismatches between the measured and the predicted velocity vectors in the reflector region indicates that the more efforts are needed to establish adequate turbulent model and the associated wall treatments.

References

1. R.G. Huget, J.K. Szymanski, and W.I. Midvidy, “Status of Physical and Numerical Modelling of CANDU Moderator Circulation,” Proceedings of 10th Annual Conference of the Canadian Nuclear Society, Ottawa, 1989.
2. R.G. Huget, J.K. Szymanski, and W.I. Midvidy, “Experimental and Numerical Modelling of Combined Forced and Free Convection in a Complex Geometry with Internal Heat Generation,” Proceedings of 9th International Heat Transfer Conference, 3, 327, 1990.
3. G.I. Hadaller, R.A. Fortman, J. Szymanski, W.I. Midvidy and D.J. Train, “Fricktional Pressure Drop for Staggered and In Line Tube Bank with Large Pitch to Diameter Ratio,” Preceedings of 17th CNS Conference, Federiction, New Brunswick, Canada, June 9-12, 1996.
4. C. Yoon, B.W. Rhee, and B.J. Min, “Validation of CFD Analysis Model for the Calculation of CANDU6 Moderator Temperature Distribution,” Proceedings of the KSME 2001 Fall Annual Meeting B (Korean), 499-504, Nov. 2001.
5. *CFX-4.2: Solver Manual*, CFX International, United Kingdom, December 1997.
6. N.E. Todreas and M.S. Kazimi, *Nuclear System II: Elements of Thermal Hydraulic Design*, Chap.5, Hemisphere Publishing Corporation, 1990.

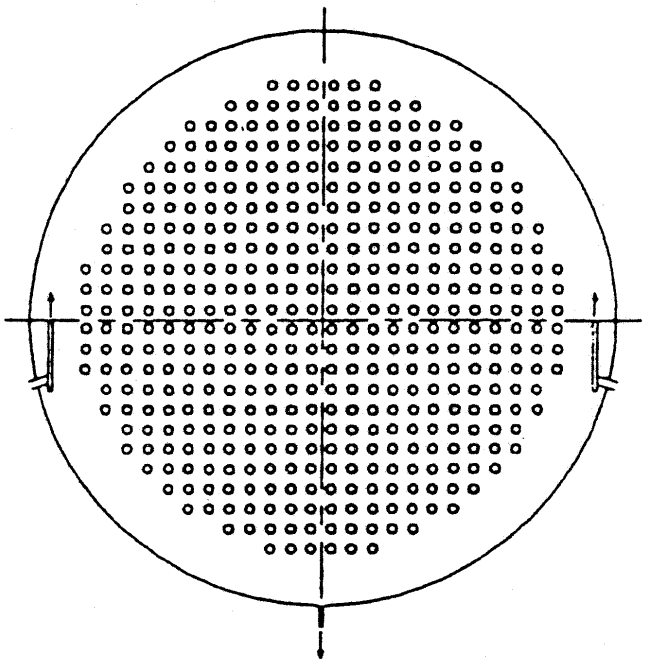

Figure 1: Test section of Stern experiments

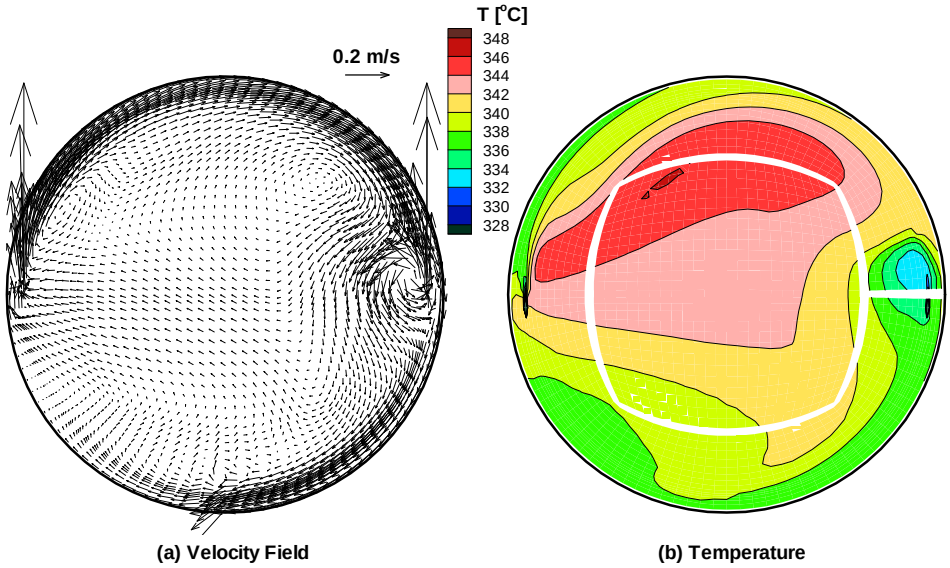

Figure 2: Velocity field and temperature distribution of nominal condition, simulated by CFX-4; total flow rate = 2.4 kg/s, inlet temperature = 55^{o}C, inlet velocity = 1 m/s, and power = 100 kW.

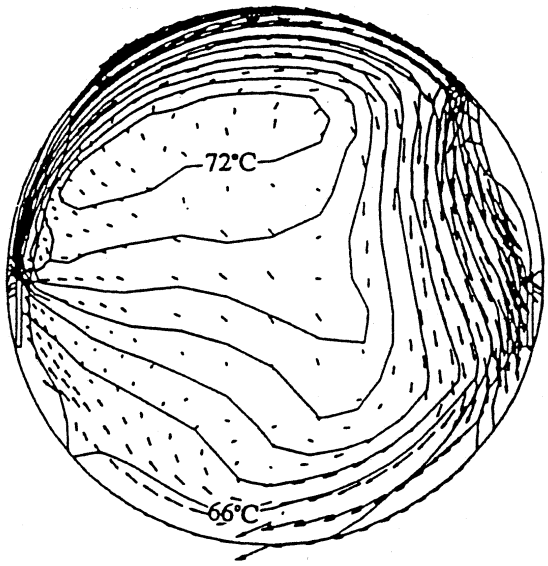

Figure 3: Velocity field and temperature distribution of nominal condition, simulated by MODTURC_CLAS; total flow rate = 2.4 kg/s, inlet temperature = 55^{o}C, inlet velocity = 1 m/s, and power = 100 kW.

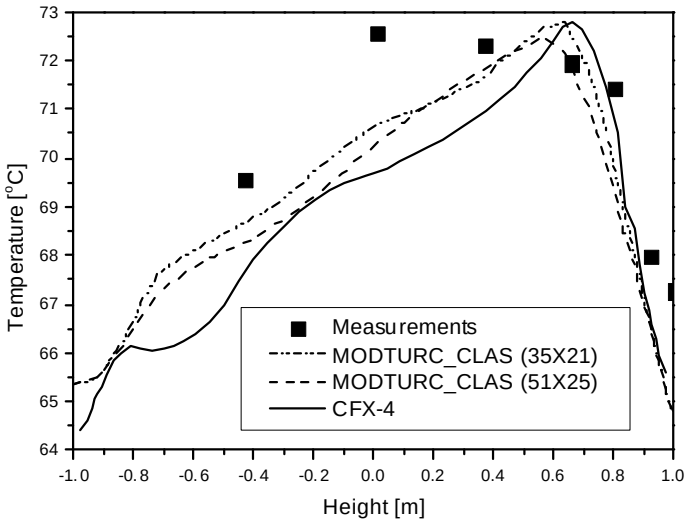

Figure 4: Temperatures at the vertical centerline in the nominal-condition test

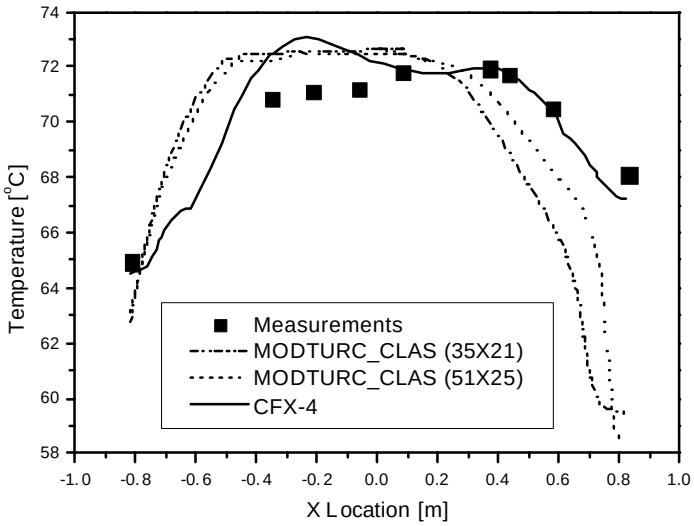

Figure 5: Temperatures at a horizontal line (Y=0.57 m) in the nominal-condition test

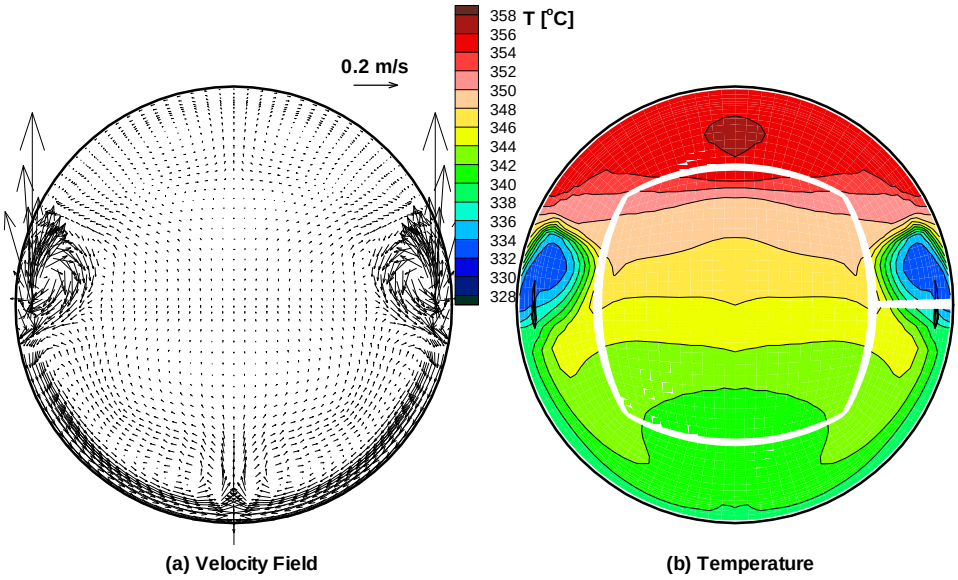

Figure 6: Velocity field and temperature distribution of low-flow condition, simulated by CFX-4; total flow rate = 2.18 kg/s, inlet temperature = 55°C, inlet velocity = 1 m/s and power = 100 kW.

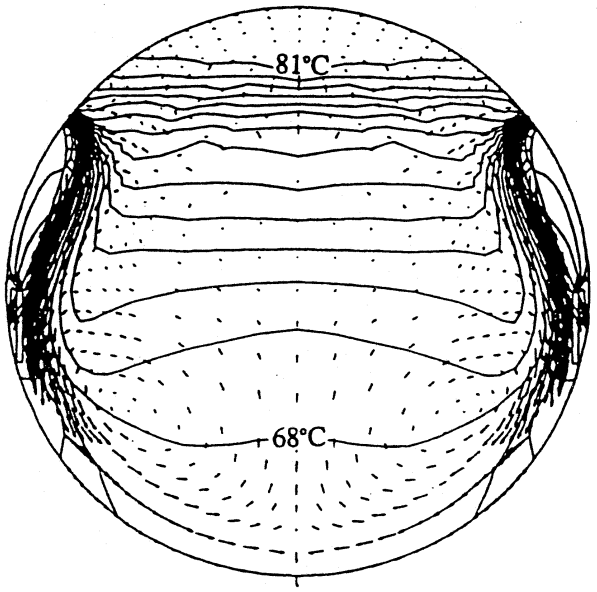

Figure 7: Velocity field and temperature distribution of low-flow condition, simulated by MODTURC_CLAS; total flow rate = 2.0 kg/s, inlet temperature = 55^{o}C, inlet velocity = 1 m/s, and power = 100 kW.